

See discussions, stats, and author profiles for this publication at: <https://www.researchgate.net/publication/373398582>

# Hydroxysafflor yellow A protects against thioacetamide-induced liver fibrosis in rats via suppressing proinflammatory/fibrogenic mediators and promoting hepatic stellate cell senes...

Article · August 2023

DOI: 10.4103/2221-1691.383689

CITATIONS

0

READS

13

8 authors, including:



Sayed Seif el-Din

Theodor Bilharz Research Institute, Warak El-Hadar, Imbaba P.O. Box 30, Giza 124...

53 PUBLICATIONS 941 CITATIONS

SEE PROFILE



Olfat Hammam

Theodor Bilharz Research Institute

182 PUBLICATIONS 2,220 CITATIONS

SEE PROFILE



Shahira M. Ezzat

Cairo University

201 PUBLICATIONS 3,734 CITATIONS

SEE PROFILE



Samira Saleh

Cairo University

105 PUBLICATIONS 1,629 CITATIONS

SEE PROFILE

Some of the authors of this publication are also working on these related projects:



Herbal formulations in experimentally-induced arthritis [View project](#)



Herbal Drugs Development into Pharmaceutical Products [View project](#)



## Original Article

## Asian Pacific Journal of Tropical Biomedicine



apjtb.org

doi: 10.4103/2221-1691.383689

Impact Factor® 1.7

## Hydroxysafflor yellow A protects against thioacetamide-induced liver fibrosis in rats *via* suppressing proinflammatory/fibrogenic mediators and promoting hepatic stellate cell senescence and apoptosis

Sayed H. Seif el-Din<sup>1</sup>✉, Olfat A. Hammam<sup>2</sup>, Shahira M. Ezzat<sup>3,4</sup>, Samira Saleh<sup>5</sup>, Marwa M. Safar<sup>5,6</sup>, Walaa H. El-Maadawy<sup>1</sup>, Naglaa M. El-Lakkany<sup>1</sup>

<sup>1</sup>Pharmacology Department, Theodor Bilharz Research Institute, Warak El-Hadar, Imbaba P.O. Box 30, Giza 12411, Egypt

<sup>2</sup>Pathology Department, Theodor Bilharz Research Institute, Warak El-Hadar, Imbaba P.O. Box 30, Giza 12411, Egypt

<sup>3</sup>Pharmacognosy Department, Faculty of Pharmacy, Cairo University, Cairo 11562, Egypt

<sup>4</sup>Pharmacognosy Department, Faculty of Pharmacy, October University for Modern Sciences and Arts, Giza, Egypt

<sup>5</sup>Pharmacology and Toxicology Department, Faculty of Pharmacy, Cairo University, Cairo 11562, Egypt

<sup>6</sup>Pharmacology and Biochemistry Department, Faculty of Pharmacy, The British University in Egypt, Cairo, Egypt

### ABSTRACT

**Objective:** To evaluate the effect of hydroxysafflor yellow A (HSYA) on thioacetamide-induced liver fibrosis.

**Methods:** Thioacetamide was administered to rats intraperitoneally in doses of 200 mg/kg twice a week for 12 weeks. Thioacetamide-intoxicated rats were given silymarin (50 mg/kg) or HSYA (5 mg/kg) orally every day for 8 weeks. Liver enzymes, fibrosis markers, histological changes as well as immunohistochemistry of TNF- $\alpha$ , IL-6, p21,  $\alpha$ -SMA, and caspase-3 were examined. The effect of HSYA on HSC-T6 activation/proliferation and apoptosis was also determined *in vitro*.

**Results:** HSYA decreased liver enzymes, TNF- $\alpha$ , IL-6, and p21 expressions, hepatic PDGF-B, TIMP-1, TGF- $\beta$ 1, and hydroxyproline levels, as well as fibrosis score (S2 *vs.* S4) compared to the thioacetamide group. HSYA also downregulated  $\alpha$ -SMA while increasing caspase-3 expression. Surprisingly, at 500  $\mu$ g/mL, HSYA had only a slightly suppressive effect on HSC proliferation, with a 9.5% reduction. However, it significantly reduced TGF- $\beta$ 1, inhibited  $\alpha$ -SMA expression, induced caspase-3 expression, and promoted cell senescence.

**Conclusions:** HSYA may be a potential therapeutic agent for delaying and reversing the progression of liver fibrosis. More research on HSYA at higher doses and for a longer period is warranted.

**KEYWORDS:** Hydroxysafflor yellow A; Thioacetamide; Hepatic stellate cells; Inflammatory markers; Liver fibrosis; p21;  $\alpha$ -SMA; Apoptosis

### 1. Introduction

Liver fibrosis is linked with the progression of chronic liver diseases regardless of etiology, including hepatitis infections caused by viruses, alcohol intake, and metabolic-associated fatty liver disease. It frequently causes liver damage, inflammation, and cell death[1]. Liver fibrosis is a common and widespread clinical

#### Significance

Liver fibrosis is a common clinical disease that can progress to liver cancer. Hydroxysafflor yellow A (HSYA) has a wide range of pharmacological activities. However, its antifibrotic effects on liver fibrosis are still completely unverified. Thus, this study sheds light on the protective mechanisms of HSYA against liver fibrosis. HSYA ameliorated hepatic fibrosis in rats by decreasing inflammatory and fibrosis markers, as well as inhibiting HSC activation. However, more studies on HSYA at higher doses and for a longer period are needed.

✉To whom correspondence may be addressed. E-mail: s.seifeldin@tbri.gov.eg; sayedseifeldin@hotmail.com

This is an open access journal, and articles are distributed under the terms of the Creative Commons Attribution-Non Commercial-ShareAlike 4.0 License, which allows others to remix, tweak, and build upon the work non-commercially, as long as appropriate credit is given and the new creations are licensed under the identical terms.

**For reprints contact:** reprints@medknow.com

©2023 Asian Pacific Journal of Tropical Biomedicine Produced by Wolters Kluwer-Medknow.

**How to cite this article:** Seif el-Din SH, Hammam OA, Ezzat SM, Saleh S, Safar MM, El-Maadawy WH, et al. Hydroxysafflor yellow A protects against thioacetamide-induced liver fibrosis in rats *via* suppressing proinflammatory/fibrogenic mediators and promoting hepatic stellate cell senescence and apoptosis. Asian Pac J Trop Biomed 2023; 13(8): 348-358.

**Article history:** Received 22 May 2023; Revision 27 June 2023; Accepted 27 July 2023; Available online 23 August 2023

condition that can develop into cirrhosis or liver cancer and kills over one million people each year, making it the 11th leading cause of death worldwide[2]. When the liver is injured, a wide spectrum of cells contribute to hepatic fibrogenesis, but activated hepatic stellate cells (HSCs) are the major effector cells that undergo trans-differentiation, transforming them from a quiescent to a proliferative and contractile myofibroblast phenotype. Furthermore, in chronic injury settings, prolonged HSC activation disrupts the buildup and disintegration of the extracellular matrix (ECM), and promotes the secretion of inflammatory cytokines and growth factors such as tumor necrosis factor- $\alpha$  (TNF- $\alpha$ ), interleukin-6 (IL-6), and transforming growth factor- $\beta$  (TGF- $\beta$ ), all of which play a driving role in HSC activation, leading to further worsening of liver fibrosis[3]. The key strategies that may aid in the elimination of activated HSCs are the reversion to a quiescent phenotype, blocking ECM synthesis, as well as promoting ECM breakdown, apoptosis, and senescence[4-6]. In chronic liver disease, Aravinthan and Alexander[7] discovered a strong spatial connection between hepatocyte senescence and activation of HSCs. Cellular senescence is a physiological mechanism in which a growing cell gets a stable cell cycle arrest in response to damage or stress, limiting cell growth. It is regulated by p21, a universal cell cycle inhibitor[8].

Despite significant advances in understanding the mechanisms underlying liver fibrosis pathogenesis during the last two decades, current therapeutic approaches remain relatively ineffectual, particularly in advanced liver fibrosis. Preclinical evidence suggests that the mechanism of liver scarring is malleable and reversible rather than unidirectional and permanent[9]. As a result, novel approaches to preventing, halting, or even reversing liver fibrosis or cirrhosis are urgently required. Natural compounds have emerged as one of the most important and major suppliers of anti-fibrosis drugs in recent years, owing to their low cost and ease of access[10]. Numerous investigations have found that naturally occurring substances such as terpenoids, phenols, alkaloids, and other phytochemicals, as well as raw extracts or isolated compounds from plants, can treat different fibrosis disorders *in vitro* and *in vivo*[10]. Hydroxysafflower yellow A (HSYA), a major natural component isolated from safflower (*Carthamus tinctorius* L.), has considerable pharmacological properties that include anti-inflammatory, antioxidant, anticoagulant, and anticancer effects[11]. Moreover, HSYA could protect against acute kidney injury[12] and lower the degree of oxidative stress in a rat model with renal ischemia-reperfusion injury[13]. To the best of the author's knowledge, only a few studies have shown that HSYA could protect rat liver from CCl<sub>4</sub>-mediated fibrogenesis[14-16]. However, its mechanisms, which primarily focus on the inhibition of HSC function, have not been thoroughly investigated. Furthermore, the role of HSYA in modulating the p21, a hepatocyte senescence marker, has yet to be reported. In the present study, we evaluated the effects of HSYA on thioacetamide (TAA)-induced liver fibrosis. Furthermore, its underlying mechanisms were investigated *in vitro*, particularly in relation to HSC proliferation, activation, and apoptosis.

## 2. Materials and methods

### 2.1. Plant materials

Flowers of *Carthamus tinctorius* L. were collected from the Experimental Station of Medicinal, Aromatic, and Poisonous Plants, Pharmacognosy Department, Faculty of Pharmacy, Cairo University, Egypt. It was kindly authenticated in the herbarium of Faculty of Science, Cairo University, Egypt. The voucher sample (03-2014) was stored in the herbarium of the Pharmacognosy Department, Faculty of Pharmacy, Cairo University, Egypt.

### 2.2. Chromatographic analysis

Thin-layer chromatography (silica gel GF254 precoated plates-Fluka) was performed with the following solvent system: ethyl acetate-methanol-water-formic acid (10:1.6:1.2:1 *v/v*) on Diaion HP-20 AG and Sephadex LH-20 (Pharmacia Fine Chemicals AB, Uppsala, Sweden). Chromatograms were captured using UV light (at 254 and 366 nm) with or without exposure to ammonia vapor. <sup>13</sup>C-NMR (100 MHz) and <sup>1</sup>H-NMR (400 MHz) were measured using Bruker NMR. The NMR spectra were detected in dimethyl sulfoxide and CD<sub>3</sub>OD. The chemical shifts are expressed in  $\delta$  (ppm) compared to an internal standard TMS.

### 2.3. Isolation and extraction of HSYA

*Carthamus tinctorius* L. air-dried flowers (2.5 kg) were powdered and extracted with distilled water (2  $\times$  10 L) for 1 h at 60°C. The extract was filtered, and the water was evaporated under low pressure to obtain 175 g of dried residue. The residue was dissolved in 1 L methanol, before being chromatographed on a diaion HP-20 AG (500 g) column. Elution started with water, then methanol-water (50%), and lastly methanol (100%). A rotary evaporator was used in each case to evaporate the solvent, providing solid residues weighing 100 g, 35 g, and 10 g, respectively. The water fraction (50 g) was chromatographed several times with ethanol-water (1:1 *v/v*) using Sephadex LH-20 (Pharmacia Fine Chemicals AB, Uppsala, Sweden) to produce orange needle-like crystals, *R*<sub>f</sub> 0.35, and mp 184.2°C of HSYA (5 g).

### 2.4. Animals

Forty adult Sprague-Dawley male rats weighing 250-300 g were purchased from the Theodor Bilharz Research Institute animal house, Giza, Egypt, and accommodated in an ecologically maintained room (20-22°C, 12 h light/dark cycles, and 50%-60% humidity) throughout the experimental periods, with free access to food and water.

## 2.5. Experimental groups and treatment

After a week of acclimatization, rats were divided into four groups of ten rats each, as follows: Normal control group (I); TAA-intoxicated group (II); silymarin (III), and HSYA (IV) treated groups. Except for the control group, all rats received TAA intraperitoneally (*i.p.*) in dosages of 200 mg/kg twice a week for 12 weeks[17]. Meanwhile, silymarin (50 mg/kg)[18] or HSYA (5 mg/kg)[14] were given orally every day for 8 weeks starting on the fifth week after TAA intoxication, where an evident stage of fibrosis (S2) was confirmed by histological analysis of hepatic tissues. All rats were euthanized by rapid decapitation under thiopental anesthesia (50 mg/kg, *i.p.*) 48 h following the end of treatment. Each rat's blood was taken in a non-heparinized glass centrifuge tube and centrifuged at 1800  $\times g$  for 15 min to separate the serum. In addition, livers were removed, weighed, and separated into two sections, the first of which was immersed in formalin for histological and immunohistochemical analyses. The remaining portion was washed with 0.9% ice-cold saline and stored at  $-80^{\circ}\text{C}$  for determination of oxidative and fibrotic markers.

## 2.6. Assay of biochemical markers

Spectrophotometric assessments of serum alanine aminotransferase (ALT) and aspartate aminotransferase (AST) (Spectrum, Egypt), as well as reduced glutathione (GSH) and lipid peroxidation (MDA) in liver homogenates (Biodiagnostic, Egypt), were performed using commercially available kits.

## 2.7. Assay of fibrosis markers

Tissue inhibitor of metalloprotease-1 (TIMP-1), transforming growth factor- $\beta$ 1 (TGF- $\beta$ 1), and platelet-derived growth factor-B (PDGF-B) levels were measured in liver tissue homogenates using commercial kits for ELISA (R & D system, MN, USA). In liver tissue samples, the level of hydroxyproline was assessed as an indirect and sensitive index of collagen concentration[19].

## 2.8. Histological and immunohistochemical analyses

Liver specimens were preserved in 10% buffered formalin for at least 24 h before being processed and inserted into paraffin blocks. Paraffin sections were stained with hematoxylin-eosin (H&E) (4  $\mu\text{m}$  thickness) and Sirius red (20  $\mu\text{m}$  thickness) for analysis of overall liver histology and collagen distribution, respectively. Imaging analysis software (Axiovision L.E. 4.8; Carl Zeiss MicroImaging, Jena, Germany) was used to quantify collagen. The red-stained area ( $\text{mm}^2$ ) was measured in five consecutive fields ( $\times 50$ ), and the morphometric analysis of hepatic fibrosis

score was calculated using a numerical rating technique[20]. Liver sections were immunohistochemically stained with anti-rat TNF- $\alpha$ , IL-6, and p21 antibodies (Santa Cruz Biotechnology, CA, USA) at a working dilution of 1:100. In addition, using a horseradish-peroxidase complex kit (Abcam Inc, UK), liver slices were immunohistochemically stained for caspase-3 and  $\alpha$ -smooth muscle actin ( $\alpha$ -SMA). The percentage of positively stained brown cytoplasm (TNF- $\alpha$ , IL-6,  $\alpha$ -SMA, and caspase-3) in hepatocytes was examined in 10 microscopic fields at  $\times 200$  for  $\alpha$ -SMA and  $\times 400$  for the rest under Zeiss light microscope (Carl Zeiss Microscopy GmbH 07745 Jena, Germany). The percentage of positively stained brown nuclei (p21) in 1000 parenchymal and non-parenchymal liver cells was determined using Zeiss light microscopy at  $\times 400$  (Carl Zeiss Microscopy GmbH 07745 Jena, Germany).

## 2.9. Measurement of cytotoxicity of HSYA to HSCs

To test the effect of HSYA on HSC proliferation, activation, and apoptosis, HSYA was dissolved in Dulbecco's Modified Eagle Medium, and filtered through a 0.22- $\mu\text{m}$  membrane and aliquots were kept at  $-20^{\circ}\text{C}$  and protected from light. Micro cultures of  $5 \times 10^3$  HSC-T6, an immortalized rat hepatic stellate cell line (a gracious gift from Prof. Scott L. Friedman, Division of Liver Diseases, Icahn School of Medicine at Mount Sinai University, New York), were grown in 200  $\mu\text{L}$  Dulbecco's Modified Eagle Medium with 10% fetal bovine serum in 96-well tissue culture plates (Nunc, Roskilde, Denmark). After 24 h, cells were treated with various concentrations of HSYA (0-500  $\mu\text{g}/\text{mL}$ ) for 24 and 48 h, and cell survival ratios were compared to untreated cells. Each test was carried out in triplicate. The sulforhodamine B (SRB) assay was used to analyze the anti-proliferative effect of HSYA on HSCs, and the  $\text{IC}_{50}$  value was calculated. Moreover, the morphology of HSCs was examined using a phase-contrast microscope [EVOS<sup>®</sup> xl core cell culture microscope (Advanced Microscopy Group, USA)]. TGF- $\beta$ 1 concentrations in culture media (ELISA Kit) and immunocytostaining with  $\alpha$ -SMA were used to measure HSC activation, whereas caspase-3 immunocytostaining was used to determine HSC apoptosis.

## 2.10. Measurement of cytotoxicity of HSYA to hepatocytes

Primary hepatocytes were freshly extracted from rats using a two-step portal collagenase perfusion of the liver[21], and their viability was evaluated by trypan blue dye exclusion. The cytotoxicity of HSYA on isolated rat hepatocytes was determined using the thiazolyl blue tetrazolium bromide (MTT) assay, in which primary hepatocytes ( $5 \times 10^3$ ) were grown in 96-well tissue culture plates and treated with HSYA at concentrations of 0-500  $\mu\text{g}/\text{mL}$  for 24 and 48

h. MTT solution (20  $\mu$ L of 0.5 mg/mL) was added to each well and incubated for another 4 h at 37 °C. The MTT-formazan produced by live cells was quantified at 570 nm using an ELISA reader.

### 2.11. Statistical analysis

The data are presented as mean $\pm$ SEM. For statistical analysis, the one-way ANOVA test was employed, followed by Tukey's *post hoc* test for multiple comparisons (GraphPad Software, San Diego, CA, USA, version 5.03). Differences were considered significant at  $P < 0.05$ .

### 2.12. Ethical statement

All animal procedures followed the National Institutes of Health's Guide for the Care and Use of Laboratory Animals. The experimental procedures were authorized by the Research Ethics Committees of Theodor Bilharz Research Institute and the Faculty of Pharmacy at Cairo University (PT: 559). All attempts were made to manage the rats humanely, to follow ethical rules, and to use only the number of animals required to generate reliable scientific data.

## 3. Results

### 3.1. Spectroscopic data and identification of HSYA

The structure was determined using nuclear magnetic resonance and mass spectrometry HR-ESI-MS ( $m/z$ ): 611.145 ( $C_{27}H_{31}O_{16}$ ). The  $^1H$ -NMR and  $^{13}C$ -NMR data (Table 1) were matched to published data [22], and the product was verified to be HSYA. Figure 1 displays the structure of the isolated and identified HSYA.

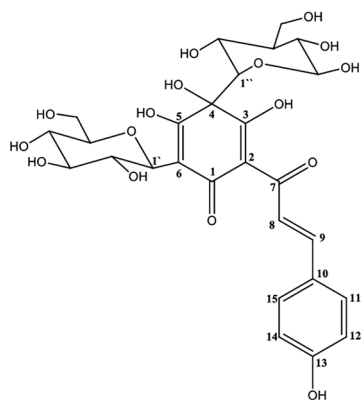


**Figure 1.** The structure of the isolated and identified hydroxysafflor yellow A (HSYA).

**Table 1.**  $^1H$ -NMR and  $^{13}C$ -NMR chemical shifts ( $\delta$  ppm) of the isolated hydroxysafflower yellow A (HSYA) (DMSO- $d_6$  for  $^1H$  400 and 100 MHz for  $^{13}C$ ).

Position	$\delta_H$ ppm (J Hz)	$\delta_C$ ppm
1	-	189.2
2	-	105.2
3	-	195.0
4	-	85.9
5	-	180.1
6	-	99.6
7	-	180.2
8	7.45 d (15)	123.2
9	7.31 d (15)	135.9
10	-	127.5
11	7.40 d (9)	129.1
12	6.77 d (9)	115.1
13	-	158.6
14	6.83 d (9)	117.1
15	7.42 d (9)	130.1
1'	3.64 d (9.5)	85.6
2'	3.35 m	69.1
3'	3.11 m	78.1
4'	2.89 m	69.5
5'	2.96 m	80.7
6'	3.37 m	60.0
1''	4.23 m	73.8
2''	4.10 m	68.5
3''	3.18 m	79.5
4''	3.12 m	70.1
5''	3.05 m	80.2
6''	3.42 m	61.6

### 3.2. Effect of HSYA on biochemical markers

In comparison to the TAA-intoxicated group, HSYA treatment reduced elevated ALT and AST levels to normal ( $P < 0.05$ ) (Figure 2A). Moreover, HSYA significantly reduced liver MDA level and normalized GSH content ( $P < 0.05$ ) (Figure 2B-C).

### 3.3. Effect of HSYA on fibrotic biomarkers

TAA markedly increased the levels of PDGF-B, TGF- $\beta$ 1, TIMP-1, and hydroxyproline in rats ( $P < 0.05$ ). HSYA treatment resulted in a considerable reduction in hepatic levels of these fibrotic biomarkers ( $P < 0.05$ ) (Figure 3).

### 3.4. Histological analysis

Histological examination of normal liver slices revealed a maintained hepatic architecture with discrete hepatic cells, sinusoidal gaps, and a central vein. Conversely, the TAA-intoxicated group displayed disturbed architecture with serious damages including sinusoidal dilatation and congestion, centrilobular necrosis, and deposition of collagen bundles surrounding the lobules, primarily in the periportal regions, resulting in thick fibrotic septae and an elevated fibrosis score of almost stage 4 (S4) (Figure 4).

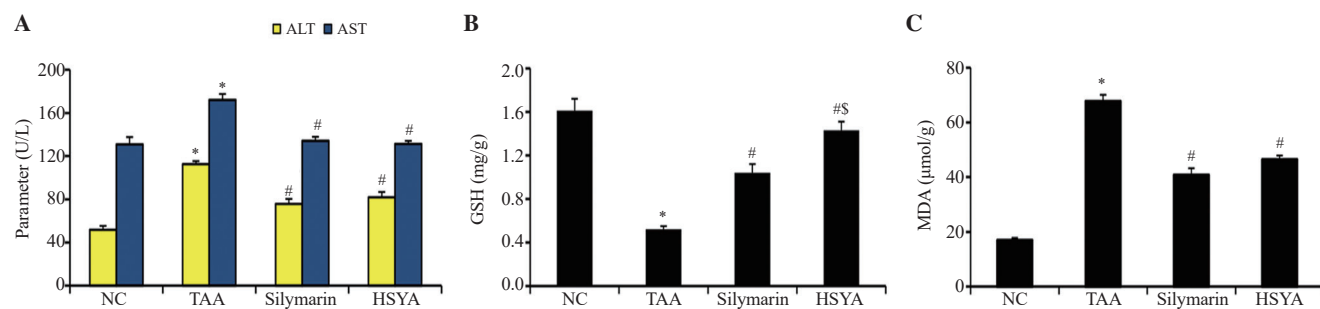


**Figure 2.** Effect of HSYA on (A) alanine aminotransferase (ALT) and aspartate aminotransferase (AST), (B) reduced glutathione (GSH), and (C) malondialdehyde (MDA) in thioacetamide (TAA)-induced fibrotic rats. Data are presented as mean  $\pm$  SEM ( $n=10$ ) and analyzed by a one-way ANOVA test followed by Tukey's *post hoc* test. \*, #, \$Significantly different from the normal control, TAA-intoxicated, and silymarin-treated groups, respectively, at  $P<0.05$ . NC: normal control.

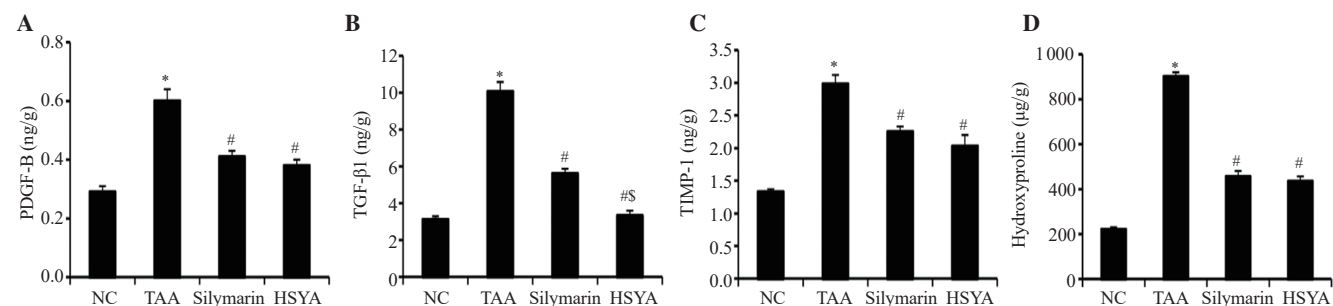


**Figure 3.** Effect of HSYA on the levels of (A) platelet-derived growth factor-B (PDGF-B), (B) transforming growth factor- $\beta$ 1 (TGF- $\beta$ 1), (C) tissue inhibitor of metalloprotease-1 (TIMP-1), and (D) hydroxyproline in liver homogenates of TAA-induced fibrotic rats. Data are expressed as mean  $\pm$  SEM ( $n=8$ ) and analyzed by a one-way ANOVA test followed by Tukey's *post hoc* test. \*, #, \$Significantly different from the normal control, TAA-intoxicated and silymarin-treated groups, respectively, at  $P<0.05$ .

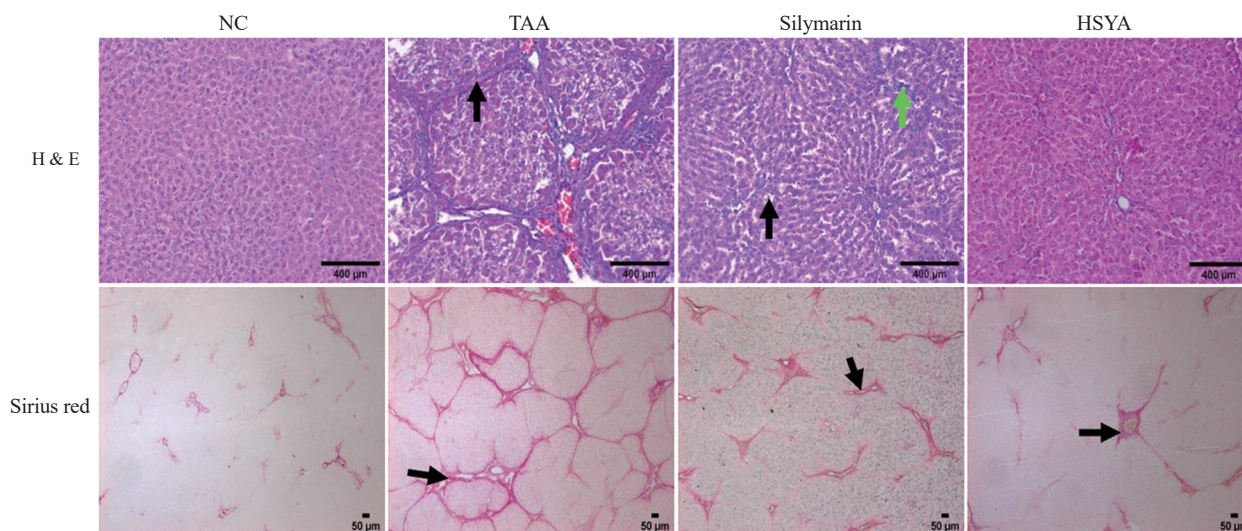


**Figure 4.** Histopathological examinations of liver sections stained with H & E ( $\times 200$ ) and Sirius red ( $\times 50$ ). In H & E figures, TAA liver sections show disruptions in architecture of the hepatic tissue (S4 stage, hepatic cirrhosis) with formation of variable-sized regenerating nodules (black arrow), silymarin-treated liver sections show an almost normal hepatic architectural pattern with mild dilation of sinusoids (black arrow) and lymphocyte infiltration (green arrow), and HSYA-treated liver sections show normal hepatic architecture. In Sirius red figures, TAA liver sections show micro and macro-cirrhotic nodules (black arrow), silymarin-treated liver sections have moderately thick fibrous bands (black arrow) and HSYA-treated liver sections have mild, thin fibrous bands (black arrow).

Administration of either silymarin or HSYA restored some of the injured hepatic tissues, as evidenced by lower levels of necrosis, fewer short collagen bundles, and S2 fibrosis scores ( $1.75 \pm 0.19$  and  $1.50 \pm 0.22$ , respectively, *vs.*  $3.63 \pm 0.21$  for the TAA group).

### 3.5. Immunohistochemical examination for proinflammatory, fibrogenic, and apoptotic markers

TNF- $\alpha$  and IL-6 expressions were negative in liver sections of normal rats (Figures 5A). However, TAA-intoxicated rats exhibited a significant rise in TNF- $\alpha$  and IL-6 (Figure 5A) expressions as evidenced by an increase in the number of positively stained brown cytoplasm of hepatic cells. TNF- $\alpha$  and IL-6 expressions were reduced by 69.77% (Figure 5B) and 73.08% (Figure 5C) in liver sections of rats treated with HSYA, respectively, as evidenced by a mild and moderate decrease in the number of positively stained brown cytoplasm of hepatic cells (Figure 5A). Notably, the extent of HSC activation in liver tissues was determined *via* immunohistochemical analysis for  $\alpha$ -SMA. Normal liver expressed  $\alpha$ -SMA in trace amounts and only in hepatic vascular smooth muscle cells of the blood vessels (Figure 6A). However, there was a

significant increase in  $\alpha$ -SMA protein expression in TAA-intoxicated hepatic tissues in areas of centrilobular and periportal fibrotic bands. In comparison to the TAA-intoxicated group, HSYA significantly lowered  $\alpha$ -SMA protein expression by 73.63% (Figure 6B).

Hepatocyte p21 expression was negligible in normal liver tissue, but it was significantly higher ( $P < 0.05$ ) in rats with TAA-induced fibrosis (Figure 6A). HSYA treatment diminished p21 expression by 72.35% (Figure 6C).

In addition, the apoptosis of HSCs was investigated using caspase-3 expression. The number of caspase-3 positive cells (apoptotic cells) observed in the control group was minimal, but it considerably increased in the TAA-intoxicated liver sections (Figure 6D). HSYA treatment enhanced caspase-3 positive cells in comparison to the TAA-intoxicated group (Figure 6D). Caspase-3 positive cells were seen in the portal and periportal regions, whereas activated HSCs deposited collagen rather than parenchymal cells (hepatocytes).

### 3.6. In vitro cytotoxicity results

Treatment with HSYA at a concentration of 500  $\mu\text{g}/\text{mL}$  had only a slightly suppressive effect on HSC proliferation at 48 h, which

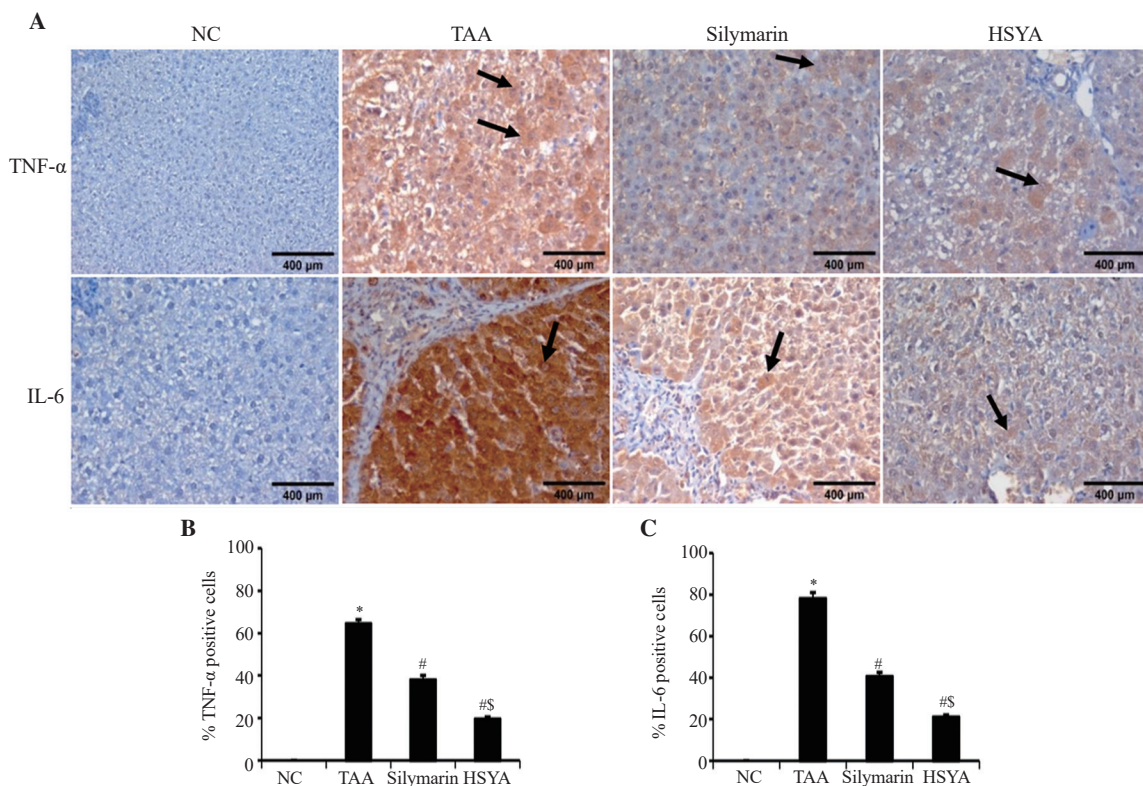


**Figure 5.** Immunohistochemical examinations of (A and B) tumor necrosis factor- $\alpha$  (TNF- $\alpha$ ;  $\times 400$ ) and (A and C) interleukin-6 (IL-6;  $\times 400$ ) in liver sections ( $n=10$ ). The expressions of TNF- $\alpha$  and IL-6 were estimated as percentage of positively stained brown cytoplasm (arrow) of hepatic cells. (B) and (C) represent the percentage of TNF- $\alpha$  and IL-6 positively stained brown cytoplasm in hepatic cells (IHC, DAB,  $\times 400$ ). Data are expressed as mean  $\pm$  SEM ( $n=10$ ) and analyzed by a one-way ANOVA test followed by Tukey's *post hoc* test. \*, #, S Significantly different from the normal control, TAA-intoxicated, and silymarin-treated groups, respectively, at  $P < 0.05$ . IHC: immunohistochemistry; DAB: 3,3'-diaminobenzidine.

did not exceed a 9.5% reduction (Figure 7A). However, HSYA morphologically extended some of the activated HSCs into flattened enlarged cells with an amplified cytoplasm-to-nucleus ratio, indicating a non-proliferative state of cell senescence (Figure 7I). In addition, it exhibited a significant decrease in TGF- $\beta$ 1 level at 500  $\mu$ g/mL when compared to untreated activated HSCs ( $P < 0.05$ ) (Figure 7C). The inhibitory impact of HSYA on HSC activation was investigated *via* determination of  $\alpha$ -SMA expression. HSYA treatment at 500  $\mu$ g/mL reduced  $\alpha$ -SMA expression (Figure 7E)

when compared to untreated cells (Figure 7D). In addition, when HSCs were incubated with HSYA, caspase-3 expression increased (Figure 7G) as compared to untreated activated cells (Figure 7F), indicating that HSYA-induced apoptosis in activated HSCs. Regarding the safety of HSYA on hepatocytes in primary culture, it showed no effect on the viability of hepatocytes at 24 and 48 h, and the viability reached approximately 90.37% at the highest concentration (500  $\mu$ g/mL), and even after prolonged exposure (Figure 7B).

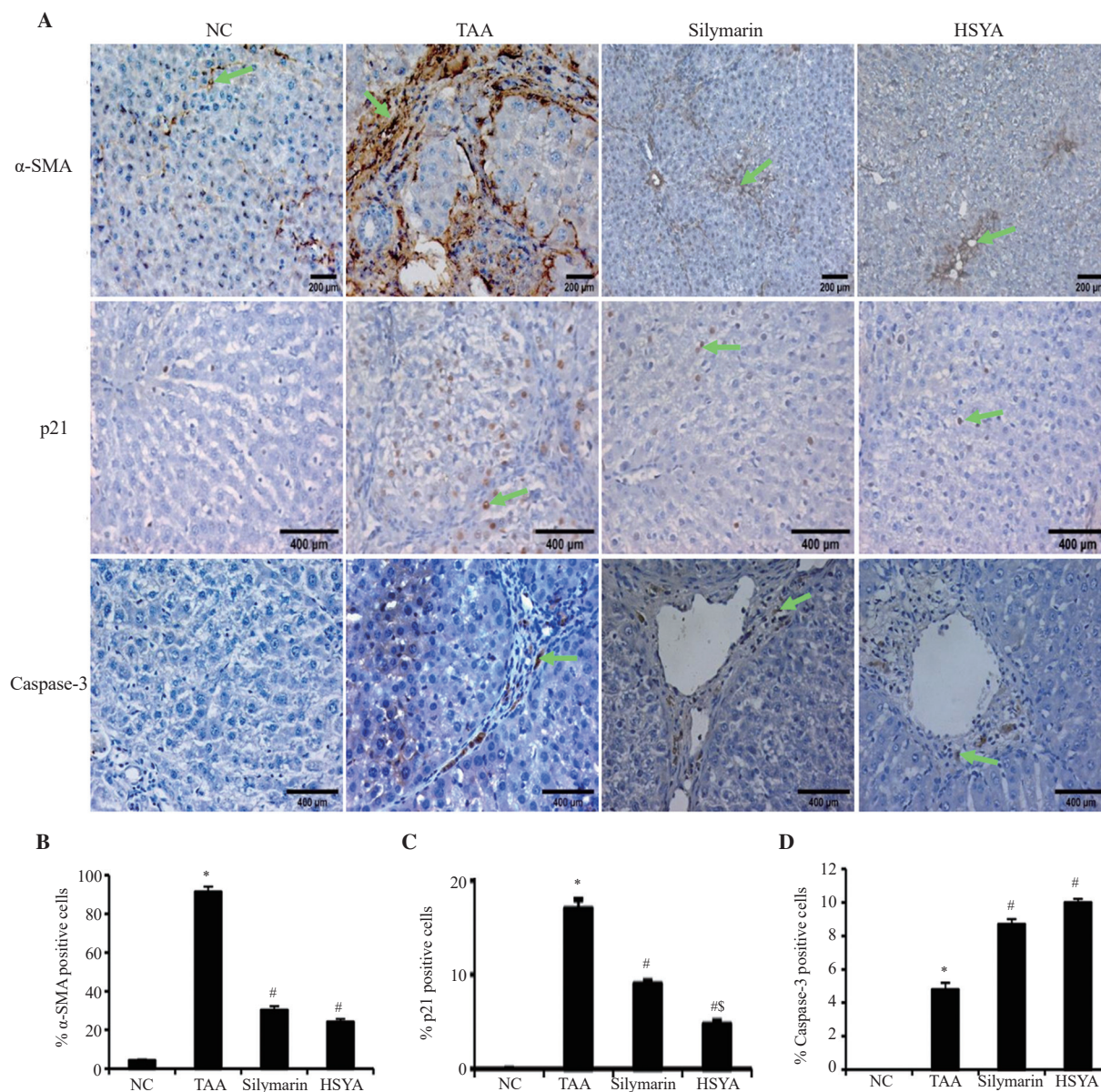


**Figure 6.** Immunohistochemical examinations of (A, B)  $\alpha$ -smooth muscle actin ( $\alpha$ -SMA), (A, C) cyclin-dependent kinase inhibitor (p21), and (A, D) caspase-3 in liver sections ( $n=10$ ). (B) represents the percentage of  $\alpha$ -SMA positively stained brown cytoplasm (arrow) of hepatic stellate cells and fibroblasts in the wall of blood vessels (IHC, DAB,  $\times 200$ ). (C) represents the percentage of p21 positively stained brown nuclei (arrow) of hepatic cells (IHC, DAB,  $\times 400$ ). (D) represents the percentage of caspase-3 positively stained brown cytoplasm (arrow) of hepatic cells in portal tracts (IHC, DAB,  $\times 400$ ). Data are expressed as mean  $\pm$  SEM ( $n=10$ ) and analyzed by a one-way ANOVA test followed by Tukey's *post hoc* test. \*, #, S Significantly different from the normal control, TAA-intoxicated and silymarin-treated groups, respectively, at  $P < 0.05$ .

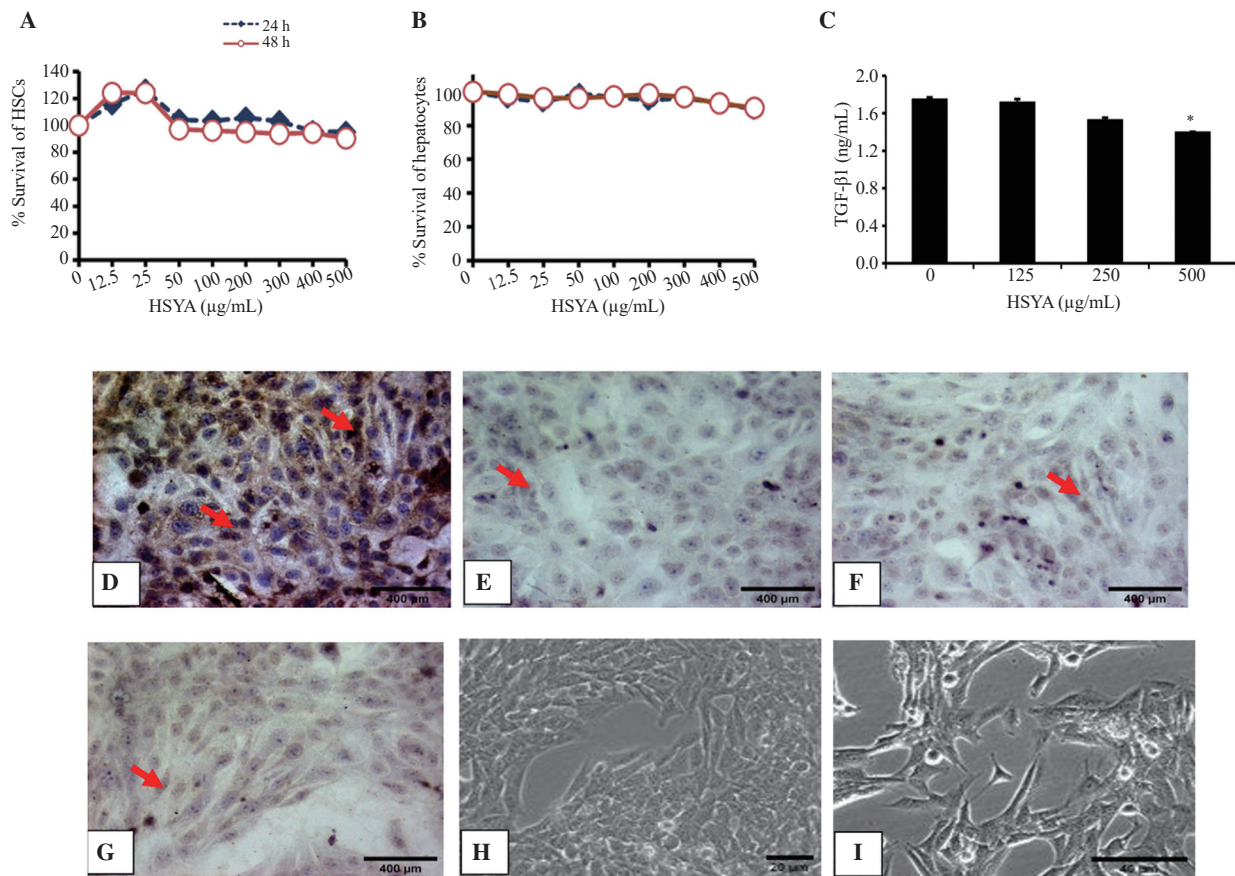


**Figure 7.** Effect of various concentrations of HSYA on (A) the proliferation and viability of hepatic stellate cells (HSCs), (B) hepatocyte viability and (C) TGF-β1 production in culture medium after 48 h. All values are represented as mean ± SEM ( $n = 3$ ) and analyzed by a one-way ANOVA test followed by Tukey's *post hoc* test. \* Significantly different from the untreated control at  $P < 0.05$ . Immunohistochemical examinations of cytospin smears ( $\times 400$ ) prepared from untreated control HSCs (D, F) and HSYA-treated cells (E, G) showing  $\alpha$ -SMA and caspase 3 immunoreactivity (arrows), respectively. The expression of  $\alpha$ -SMA and caspase 3 was estimated as the number of positively stained cells. Photomicrographs H and I illustrate the morphology of HSCs in untreated control cells (H;  $\times 20$ ) and HSYA-treated cells (I;  $\times 40$ ) under a phase-contrast microscope.

#### 4. Discussion

Liver fibrosis is a serious threat to public health that can lead to cirrhosis, cancer, and death. TAA is a thiono-sulfur substance that is commonly used to generate liver fibrosis in rats in order to examine the underlying mechanisms and therapeutic benefits of potential antifibrotic drugs[23]. It has been proven to induce reversible fibrosis in rodents comparable to that seen in humans[24], as well as various grades of liver damage in rodents including nodular cirrhosis, hepatic cell proliferation, and parenchymal cell necrosis[25]. In the current study, H & E histological analysis of chronic TAA intoxication revealed a disrupted architecture with severe damage manifested as micro and macro nodules, many fiber extensions, and collagen deposition (S4) surrounding the hepatic lobules, as well as a significant rise in hydroxyproline content. These results were supported by a noticeable rise in serum ALT and AST levels, which are deemed the most sensitive and dramatic indicators of hepatocyte injury, including cellular rupture and loss of functional cell integrity[26]. These findings suggest that rat hepatic fibrosis

has been successfully established. Furthermore, these data are associated with increased oxidative stress, which is an important driver of liver disease, as evidenced by lipid peroxidation (higher MDA), which compromises membrane integrity and causes liver damage[27], and GSH depletion. This could directly stimulate and activate HSCs, causing them to secrete profibrogenic cytokines TGF-β1 and PDGF-B and release proinflammatory cytokines TNF-α and IL-6, promoting acute liver damage to further develop into liver fibrosis. Besides, a pathogenic process driven by inflammation in the liver activates quiescent HSCs, resulting in ECM buildup, including  $\alpha$ -SMA as a hallmark of HSC activation, collagen, and TIMPs as shown herein and in other studies[17,25]. In the current study, HSYA increased hepatic GSH contents while dramatically decreasing hepatic MDA levels, as previously reported in CCl<sub>4</sub> and alcohol-induced liver injury[28]. HSYA has been shown to boost endogenous antioxidant enzyme activity, thereby speeding up the healing mechanism of the injured cell membrane[29] as shown by the recovery of raised ALT and AST levels following treatment. This demonstrates HSYA's ability to safeguard the liver from the

harmful effects of TAA by preserving the cell membrane integrity of liver cells. In this study, HSYA also had anti-inflammatory effects, as evidenced by lowered IL-6 and TNF- $\alpha$  expressions, as well as antifibrogenic effects, as confirmed by decreased  $\alpha$ -SMA, TIMP-1, TGF- $\beta$ 1, and PDGF-B as well as collagen deposition. Such findings could be explained and reinforced by *in vitro* results in which HSYA reduced TGF- $\beta$ 1 concentrations in culture media as well as the number of activated HSCs, as demonstrated by a decrease in  $\alpha$ -SMA expression. Aside from inhibiting HSC activation, HSYA reduced collagen deposition (S4 to S2) in the livers of TAA-intoxicated rats and thus could assist in the prevention of liver fibrosis progression. These findings supported the previous research[29], which found that HSYA administration significantly reduced TIMP-1 expression while increasing collagen lysis. Surprisingly, the *in vitro* proliferation results of HSYA on HSCs did not match the observed alterations in HSCs morphology or the reported reduction in HSC activation. The inability of HSYA to exert antiproliferative effects on HSCs *in vitro* has previously been reported[30], where treatment of HSCs with various concentrations of HSYA showed no significant changes in the percentages of activated HSCs in the S-phase of cell cycle progression. This could imply that exposing HSCs to greater HSYA concentrations for longer periods (72 or 96 h) may improve HSYA's antiproliferative effects on HSCs.

Importantly, HSYA treatment not only inhibited HSC activation but also induced apoptosis *in vitro* and in animal hepatic tissues, as evidenced by greater expression of caspase-3 as compared to TAA-intoxicated rats. Caspase-3 is assumed to be the principal executioner caspase during most apoptotic processes; with its activation required for both DNA fragmentation and plasma membrane blebbing[31]. The increased apoptosis may be linked to the reduced TIMP-1 concentrations and collagen deposits found in the present work and other studies[32,33]. It was reported that HSYA inhibited the activation of the extracellular signal-regulated kinase1/2 (ERK1/2)[34], causing cytochrome c release into the cytosol from mitochondria, lowering the Bcl-2/Bax ratio, and increasing caspase-3 protease activity, providing a plausible mechanism for HSYA's apoptotic-inducing effect on cultured activated HSCs[30]. Others speculated that the increase in caspase-3 expression was caused by the activation of the apoptotic intrinsic route in response to cell stress or damage, resulting in the leakage of cytochrome c into the cell cytoplasm and, eventually, the activation of caspase[35].

p21, a powerful cell cycle inhibitor, and p53 transcriptional target is required for cellular senescence induction and maintenance[36]. In chronic liver disease, a close geographical correlation between hepatocyte senescence and HSC activation was found[7,37]. However, the mechanisms underlying the association between cellular senescence and the progression of liver disease are complicated and uncertain. Herein, *in vitro* treatment of activated HSCs with HSYA changed the morphology of some HSCs into a flattened form with

enlarged cell size and an increased cytoplasm-to-nucleus ratio, which could be an indication of cell senescence. It has been reported that inducing HSC senescence could block its activation with regression of liver fibrosis, whereby senescent cells lack their role-specific to that cell type during senescence[38]. Senescence of hepatocytes, on the other hand, has been associated with fibrosis and deterioration in persistent liver disorders[37,39]. Despite the fact that hepatocytes are the most prevalent cell type in the liver, the existence of senescent cells within the fibrotic scar in the livers of both humans and mice suggested that these cells originated from activated HSCs, which proliferate immediately after liver damage and account for much of the ECM generated during fibrosis[40]. In this study, TAA-intoxicated liver sections with increased HSC activation (increased  $\alpha$ -SMA expression) were associated with higher hepatocyte p21 expression; however, in the HSYA-treated groups, areas of the liver with fewer activated HSCs (lowered  $\alpha$ -SMA expression) were associated with lower hepatocyte p21 expression. These data imply that hepatocyte senescence may be involved in the activation of stellate cells and the advancement of fibrosis. Thus, eliminating senescent hepatocytes should benefit in the therapy of senescence-related diseases. Importantly, HSYA was found to be safe on primary isolated hepatocytes at concentrations up to 500  $\mu$ g/mL and for a period of up to 48 h. These findings support previous researches that found polyphenolics preferentially trigger oxidative damage and cytotoxicity in activated HSCs while causing no cytotoxicity in hepatocytes[14,41].

The anti-inflammatory and antifibrotic efficacy of HSYA *in vivo* was compared to that of silymarin, a polyphenolic flavonoid utilized as a standard drug in this study because it is a traditional liver-protecting drug with specific efficacy[42,43]. Silymarin protects against injury from various toxic chemicals such as TAA[44] or CCl<sub>4</sub>[30], by inhibiting the production of TNF- $\alpha$ , interferon- $\gamma$ , IL-2, IL-4, and IL-6. Preclinical and clinical studies have revealed that silymarin and its flavonolignans significantly convey a broad spectrum of pharmacological activities such as antioxidant, anti-inflammatory, hepatoprotection, anti-diabetic, anti-cancer, cardioprotection, immunomodulation, and many others[45]. Notably, HSYA exceeded silymarin in terms of restoring GSH, normalizing TNF- $\alpha$  and IL-6 levels, and significantly lowering TGF- $\beta$ 1 and p21. However, it had a similar effect to silymarin in terms of caspase-3 expression.

In conclusion, HSYA demonstrated promising anti-inflammatory and antifibrotic properties. The *in vivo* and *in vitro* findings suggested that HSYA could prevent hepatic fibrosis progression by modulating inflammatory cytokines, inhibiting HSC activation, and inducing apoptosis in activated HSCs, and these effects were supported by decreased p21 hepatocyte expression, a lower fibrosis score, and observed HSC morphological changes. However, this study has some limitations. The *in vitro* anti-proliferative effects of HSYA on HSCs after 48 h did not match the observed changes in HSC

morphology or the reported reduction in HSC activation *in vitro* and *in vivo*. Therefore, this effect must be studied over a longer period with higher concentrations of HSYA. Furthermore, more detailed parameters are necessary to evaluate the senescence of HSCs *in vitro* and *in vivo*. Overall, HSYA is a potential therapeutic option for treating liver inflammation and slowing/reversing hepatic fibrosis progression.

### Conflict of interest statement

The authors declare that they have no conflicts of interest.

### Acknowledgments

The authors would like to thank Prof. S.L. Friedman, Mount Sinai School of Medicine, NY, for his gracious gift of HSC-T6 cells.

### Funding

This investigation is part of a project funded by Theodore Bilharz Research Institute (grant number: ID-MS-99/A, Principal investigator: Naglaa M. El-Lakkany).

### Authors' contributions

SHS contributed to the study's conceptualization and design, data analysis and interpretation, and critical revision of the manuscript. OAH contributed to histological and immunohistochemistry investigations. SME carried out isolation, extraction, and identification of HSYA. MMS helped with data curation and formal analysis. SS supervised the study and contributed to the final version of the manuscript. WHE contributed to the study's conceptualization, investigation of *in vitro* and *in vivo* studies, data curation and formal analysis. NME contributed to the study's conceptualization and design, funding acquisition, project administration, validation, data analysis and interpretation, drafting and critical editing/revision of the manuscript.

### References

- [1] Zhang CY, Liu S, Yang M. Treatment of liver fibrosis: Past, current, and future. *World J Hepatol* 2023; **15**(6): 755-774.
- [2] Wan SZ, Liu C, Huang CK, Luo FY, Zhu X. Ursolic acid improves intestinal damage and bacterial dysbiosis in liver fibrosis mice. *Front*

*Pharmacol* 2019; **10**. doi: 10.3389/fphar.2019.01321.

- [3] Wang FD, Zhou J, Chen EQ. Molecular mechanisms and potential new therapeutic drugs for liver fibrosis. *Front Pharmacol* 2022; **13**. doi: 10.3389/fphar.2022.787748.
- [4] Prakash J, Pinzani M. Fibroblasts and extracellular matrix: Targeting and therapeutic tools in fibrosis and cancer. *Adv Drug Deliv Rev* 2017; **1**(121): 1-2.
- [5] Yu HX, Yao Y, Bu FT, Chen Y, Wu YT, Yang Y, et al. Blockade of YAP alleviates hepatic fibrosis through accelerating apoptosis and reversion of activated hepatic stellate cells. *Mol Immunol* 2019; **1**(107): 29-40.
- [6] Huang YH, Chen MH, Guo QL, Chen ZX, Chen QD, Wang XZ. Interleukin-10 induces senescence of activated hepatic stellate cells *via* STAT3-p53 pathway to attenuate liver fibrosis. *Cell Signal* 2020; **66**. doi: 10.1016/J.CELLSIG.2019.109445.
- [7] Aravinthan AD, Alexander GJM. Senescence in chronic liver disease: Is the future in aging? *J Hepatol* 2016; **65**(4): 825-834.
- [8] González-Gualda E, Baker AG, Fruk L, Muñoz-Espín D. A guide to assessing cellular senescence *in vitro* and *in vivo*. *FEBS J* 2021; **288**(1): 56-80.
- [9] Zoubek ME, Trautwein C, Strnad P. Reversal of liver fibrosis: From fiction to reality. *Best Pract Res Clin Gastroenterol* 2017; **31**(2): 129-141.
- [10] Basso BD, Haute GV, Ortega-Ribera M, Luft C, Antunes GL, Bastos MS, et al. Methoxyeugenol deactivates hepatic stellate cells and attenuates liver fibrosis and inflammation through a PPAR-gamma and NF-κB mechanism. *J Ethnopharmacol* 2021; **280**. doi: 10.1016/j.jep.2021.114433.
- [11] Zhao F, Wang P, Jiao Y, Zhang X, Chen D, Xu H. Hydroxysafflor yellow A: A systematical review on botanical resources, physicochemical properties, drug delivery system, pharmacokinetics, and pharmacological effects. *Front Pharmacol* 2020; **11**. doi: 10.3389/fphar.2020.579332.
- [12] Bai J, Zhao J, Cui D, Wang F, Song Y, Cheng L, et al. Protective effect of hydroxysafflor yellow A against acute kidney injury *via* the TLR4/NF-κB signaling pathway. *Sci Rep* 2018; **8**(1). doi: 10.1038/S41598-018-27217-3.
- [13] Jiang S, Shi Z, Li C, Ma C, Bai X, Wang C. Hydroxysafflor yellow A attenuates ischemia/reperfusion-induced liver injury by suppressing macrophage activation. *Int J Clin Exp Pathol* 2014; **7**(5): 2595-2608.
- [14] Zhang Y, Guo J, Dong H, Zhao X, Zhou L, Li X, et al. Hydroxysafflor yellow A protects against chronic carbon tetrachloride-induced liver fibrosis. *Eur J Pharmacol* 2011; **660**(2-3): 438-444.
- [15] Liu Q, Wang CY, Liu Z, Ma XS, He YH, Chen SS, et al. Hydroxysafflor yellow A suppresses liver fibrosis induced by carbon tetrachloride with high-fat diet by regulating PPAR-γ/p38 MAPK signaling. *Pharm Biol* 2014; **52**(9): 1085-1093.
- [16] Li CC, Yang CZ, Li XM, Zhao XM, Zou Y, Fan L, et al. Hydroxysafflor yellow A induces apoptosis in activated hepatic stellate cells through ERK1/2 pathway *in vitro*. *Eur J Pharm Sci* 2012; **46**(5): 397-404.
- [17] Shirin H, Sharvit E, Aeed H, Gavish D, Bruck R. Atorvastatin and rosuvastatin do not prevent thioacetamide induced liver cirrhosis in rats.

- World J Gastroenterol* 2013; **19**(2): 241-248.
- [18]Kadir FA, Kassim NM, Abdulla MA, Yehye WA. Hepatoprotective role of ethanolic extract of *Vitex negundo* in thioacetamide-induced liver fibrosis in male rats. *Evid Based Complement Alternat Med* 2013; **2013**. doi: 10.1155/2013/739850.
- [19]Woessner JF. The determination of hydroxyproline in tissue and protein samples containing small proportions of this imino acid. *Arch Biochem Biophys* 1961; **93**(2): 440-447.
- [20]Li L, Hu Z, Li W, Hu M, Ran J, Chen P, et al. Establishment of a standardized liver fibrosis model with different pathological stages in rats. *Gastroenterol Res Pract* 2012; **2012**. doi: 10.1155/2012/560345.
- [21]Seglen PO. Preparation of isolated rat liver cells. *Methods Cell Biol* 1976; **13**: 29-83.
- [22]Bai Y, Lu P, Han C, Yu C, Chen M, He F, et al. Hydroxysafflor yellow A (HSYA) from flowers of *Carthamus tinctorius* L. and its vasodilatation effects on pulmonary artery. *Molecules* 2012; **17**(12): 14918-14927.
- [23]Al-Attar AM, Alrobai AA, Almalki DA. Effect of *Olea oleaster* and *Juniperus procera* leaves extracts on thioacetamide induced hepatic cirrhosis in male albino mice. *Saudi J Biol Sci* 2016; **23**(3): 363-371.
- [24]Nascimento M, Piran R, Da Costa RM, Giordani MA, Carneiro FS, Aguiar DH, et al. Hepatic injury induced by thioacetamide causes aortic endothelial dysfunction by a cyclooxygenase-dependent mechanism. *Life Sci* 2018; **212**: 168-175.
- [25]Salama SM, Abdulla MA, AlRashdi AS, Ismail S, Alkiyumi SS, Golbabapour S. Hepatoprotective effect of ethanolic extract of *Curcuma longa* on thioacetamide induced liver cirrhosis in rats. *BMC Complement Altern Med* 2013; **13**. doi: 10.1186/1472-6882-13-56.
- [26]Yang CC, Fang JY, Hong TL, Wang TC, Zhou YE, Lin TC. Potential antioxidant properties and hepatoprotective effects of an aqueous extract formula derived from three Chinese medicinal herbs against CCL<sub>4</sub>-induced liver injury in rats. *Int Immunopharmacol* 2013; **15**: 106-113. doi: 10.1016/j.intimp.2012.10.017.
- [27]Shay JES, Hamilton JP. Hepatic fibrosis: Avenues of investigation and clinical implications. *Clin Liver Dis (Hoboken)* 2018; **11**(5): 111-114.
- [28]He Y, Liu Q, Li Y, Yang X, Wang W, Li T, et al. Protective effects of hydroxysafflor yellow A (HSYA) on alcohol-induced liver injury in rats. *J Physiol Biochem* 2015; **71**(1): 69-78.
- [29]Wang CY, Liu Q, Huang QX, Liu JT, He YH, Lu JJ, et al. Activation of PPAR $\gamma$  is required for hydroxysafflor yellow A of *Carthamus tinctorius* to attenuate hepatic fibrosis induced by oxidative stress. *Phytomedicine* 2013; **20**(7): 592-599.
- [30]Li CC, Yang CZ, Li XM, Zhao XM, Zou Y, Fan L, et al. Hydroxysafflor yellow A induces apoptosis in activated hepatic stellate cells through ERK1/2 pathway *in vitro*. *Eur J Pharm Sci* 2012; **46**(5): 397-404.
- [31]Park EJ, Zhao YZ, Kim YC, Sohn DH. Bakuchiol-induced caspase-3-dependent apoptosis occurs through c-Jun NH2-terminal kinase-mediated mitochondrial translocation of Bax in rat liver myofibroblasts. *Eur J Pharmacol* 2007; **559**(2-3): 115-123.
- [32]Liu XW, Bernardo MM, Fridman R, Kim HRC. Tissue inhibitor of metalloproteinase-1 protects human breast epithelial cells against intrinsic apoptotic cell death *via* the focal adhesion kinase/phosphatidylinositol 3-kinase and MAPK signaling pathway. *J Biol Chem* 2003; **278**(41): 40364-40372.
- [33]Friedman SL. Evolving challenges in hepatic fibrosis. *Nat Rev Gastroenterol Hepatol* 2010; **7**(8): 425-436.
- [34]Choi JH, Hwang YP, Park BH, Choi CY, Chung YC, Jeong HG. Anthocyanins isolated from the purple-fleshed sweet potato attenuate the proliferation of hepatic stellate cells by blocking the PDGF receptor. *Environ Toxicol Pharmacol* 2011; **31**(1): 212-219.
- [35]Kubli DA, Gustafsson ÅB. Mitochondria and mitophagy: The yin and yang of cell death control. *Circ Res* 2012; **111**(9): 1208-1221.
- [36]Campisi J, D'Adda Di Fagagna F. Cellular senescence: When bad things happen to good cells. *Nat Rev Mol Cell Biol* 2007; **8**(9): 729-740.
- [37]Aravinthan A, Pietrosi G, Hoare M, Jupp J, Marshall A, Verrill C, et al. Hepatocyte expression of the senescence marker p21 is linked to fibrosis and an adverse liver-related outcome in alcohol-related liver disease. *PLoS One* 2013; **8**(9). doi: 10.1371/JOURNAL.PONE.0072904.
- [38]Klein S, Klösel J, Schierwagen R, Körner C, Granzow M, Huss S, et al. Atorvastatin inhibits proliferation and apoptosis, but induces senescence in hepatic myofibroblasts and thereby attenuates hepatic fibrosis in rats. *Lab Invest* 2012; **92**(10): 1440-1450.
- [39]Nakajima T, Nakashima T, Okada Y, Jo M, Nishikawa T, Mitsumoto Y, et al. Nuclear size measurement is a simple method for the assessment of hepatocellular aging in non-alcoholic fatty liver disease: Comparison with telomere-specific quantitative FISH and p21 immunohistochemistry. *Pathol Int* 2010; **60**(3): 175-183.
- [40]Wiemann SU, Satyanarayana A, Tshuridu M, Tillmann HL, Zender L, Klempnauer J, et al. Hepatocyte telomere shortening and senescence are general markers of human liver cirrhosis. *FASEB J* 2002; **16**(9): 935-942.
- [41]Chang YJ, Hsu SL, Liu YT, Lin YH, Lin MH, Huang SJ, et al. Gallic acid induces necroptosis *via* TNF- $\alpha$  signaling pathway in activated hepatic stellate cells. *PLoS One* 2015; **10**(3). doi: 10.1371/JOURNAL.PONE.0120713.
- [42]Neha ASJ, Singh N. Silymarin and its role in chronic diseases. *Adv Exp Med Biol* 2016; **929**: 25-44.
- [43]Federico A, Dallio M, Loguercio C. Silymarin/silybin and chronic liver disease: A marriage of many years. *Molecules* 2017; **22**(2). doi: 10.3390/MOLECULES22020191.
- [44]Ghosh S, Sarkar A, Bhattacharyya S, Sil PC. Silymarin protects mouse liver and kidney from thioacetamide induced toxicity by scavenging reactive oxygen species and activating PI3K-Akt pathway. *Front Pharmacol* 2016; **7**. doi: 10.3389/FPHAR.2016.00481.
- [45]Wadhwa K, Pahwa R, Kumar M, Kumar S, Sharma PC, Singh G, et al. Mechanistic insights into the pharmacological significance of silymarin. *Molecules* 2022; **27**(16). doi: 10.3390/MOLECULES27165327.

## Publisher's note

The Publisher of the *Journal* remains neutral with regard to jurisdictional claims in published maps and institutional affiliations.